ECE ILLINOIS

ILLINOIS

Observation of Tsunami-Generated Ionospheric Signatures in Hawaii from the 16 September 2015 Illapel Earthquake

Matthew A. Grawe[1], Jonathan J. Makela[1]

[1]Department of Electrical and Computer Engineering, University of Illinois at Urbana-Champaign

Abstract

Tsunamis generate internal gravity waves (IGWs) that propagate vertically into the atmosphere, and can create detectable signatures in the ionosphere. These signatures have consistently been observed in the presence of a tsunami for over a decade in the total electron content and for over five years in the 630.0 nm airglow. Here, we show perturbations appearing in filtered GPS-derived total electron content (TEC) and 630.0-nm airglow above Hawaii during the passing of the tsunami induced by the 16 September, 2015 earthquake in Illapel, Chile. We report measurements of IGW parameters from both observation methodologies using a combination of prior methods and a newer method that uses a Gabor filter bank. A previously developed geometric model that takes into account the posture of tsunami-induced IGW in the geomagnetic field and the observation geometry is shown to predict fairly well the expected location of the observation in the sky. Results are also compared to signatures from the March 2011 Tohoku event.

Background

- Tsunamis locally modulate the height of the ocean surface as they travel, seeding internal gravity waves at the bottom of the atmosphere.
- These internal gravity wave packets eventually reach the ionosphere, perturbing the ion and electron densities and generating a signature in the airglow and TEC.
- The dependence of the neutral-ion coupling process on the geomagnetic field direction and the observation geometry introduces anisotropy into the airglow and TEC measurement, typically inducing a stronger signature downstream of the tsunami [2].

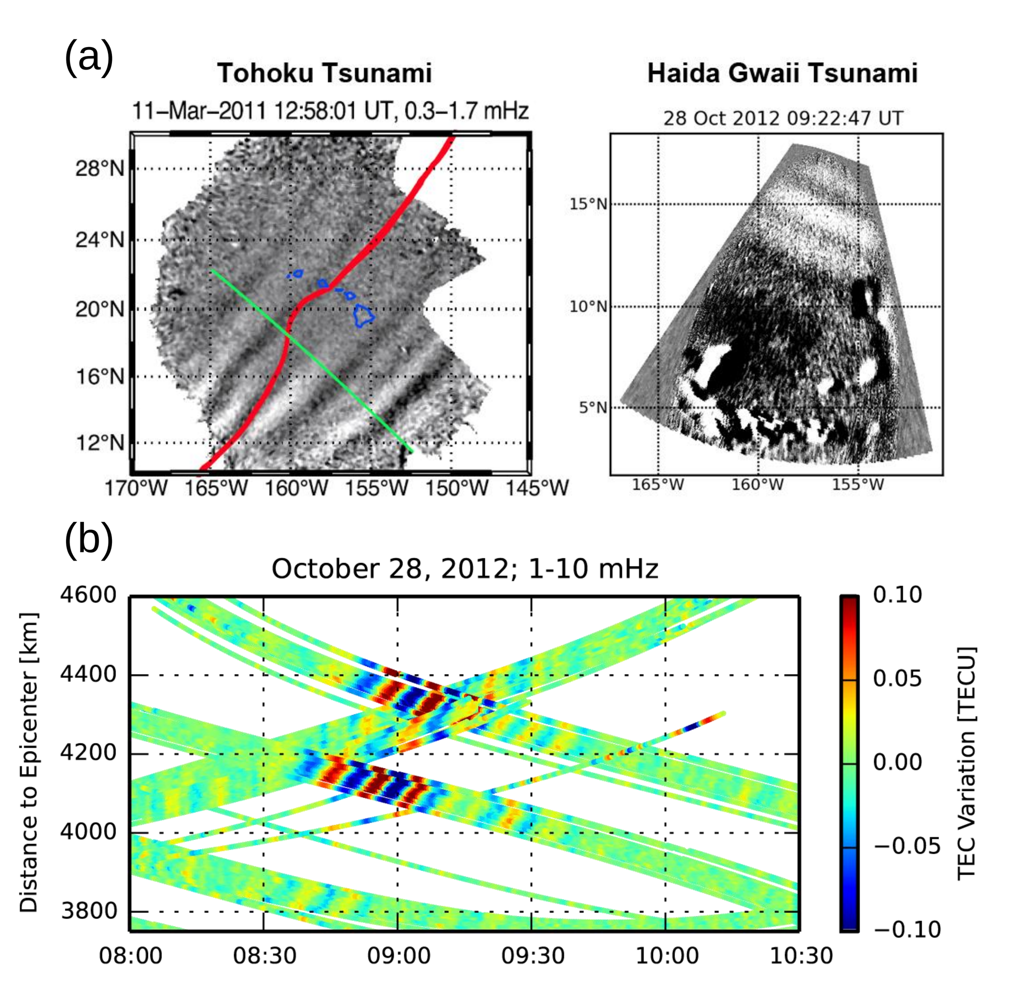

Fig. 1 (a) Temporally filtered 630.0-nm airglow images showing tsunami-generated signatures appearing in airglow images from the 11 March 2011 Tohoku [1] and 28 October 2012 Haida Gwaii tsunami events [2]. (b) Temporally filtered TEC shown as a hodochrone for the 28 October 2012 Haida Gwaii event. The slope of the red bands is the propagation speed away from the epicenter.

References

[1] J. J. Makela, P. Lognonne, H. Hebert, T. Gehrels, L. Rolland, S. Allgeyer, A. Kherani, G. Occhipinti, E. Astafyeva, P. Cosson, A. Loevenbruck, E. Clevede, M. C. Kelley, and J. Lamouroux. Imaging and modeling the ionospheric airglow response over Hawaii to the tsunami generated by the Tohoku earthquake of 11 March 2011. Geophys. Res. Lett., 38(24) jul 2011.

[2] Matthew A. Grawe and Jonathan J. Makela. The ionospheric responses to the 2011 Tohoku 2012 Haida Gwaii, and 2010 Chile tsunamis: Effects of tsunami orientation and observation geometry. Earth and Space Science, 2(11):472-483, nov 2015.

[3] Movellan, J. R. (1996), Tutorial on Gabor Filters. http://read.pudn.com/downloads140/ebook/603229/gabor.pdf

Acknowledgements

Work at the University of Illinois at Urbana-Champaign was supported by the Office of Naval Research grant N00014-13-1-0350. We acknowledge valuable discussions on parts of this poster within the International Space Science Institute (ISSI) team called “Understanding Solid Earth/Ocean-Ionosphere Coupling: Improving Models and Observational Capabilities for Monitoring Tsunamis from Space”. We thank DART/NOAA and UNAVCO for data collection. The continued operation of the CNFI and CASI instruments on Mount Haleakala would not be possible without the on-site support of Jacob Burger. We thank Professor Michael C. Kelley for making the CASI and CNFI data available for our use. Data from CASI used in this study is available upon request from Jonathan Makela (jmakela@illinois.edu).

Parameter Measurement Methods

- We measured phase speed directly by tracing the path of the wavefront over several airglow frames.
- Wavelength and orientation were measured as the argmax over wavelength and orientation using energy surfaces generated by passing temporally filtered airglow frames through a Gabor filter bank. Mathematically,

$$\hat{\lambda},\, \hat{\theta} = \underset{\lambda_l,\, \theta_k}{\operatorname{argmax}} ||\mathbf{X} * \mathbf{g}_{kl}(\lambda_l, \theta_k)||_F$$

where

$$g_{kl}(\mathbf{x}) = \frac{e^{-\frac{1}{2}\mathbf{x}^T\mathbf{A}_{kl}\mathbf{x}+j\mathbf{k}_{kl}^T\mathbf{x}}}{2\pi\sigma_x\sigma_y} - L_{kl}\frac{e^{-\frac{1}{2}\mathbf{x}^T\mathbf{D}_{kl}\mathbf{x}}}{2\pi\sigma_x\sigma_y}$$

$$L_{kl} = e^{-\frac{1}{2}\mathbf{k}_{kl}^T\mathbf{A}_{kl}^{-T}\mathbf{k}_{kl}} \qquad \mathbf{k}_{kl} = \frac{2\pi}{\lambda_{kl}}\begin{bmatrix}\cos\theta_{kl}\\ \sin\theta_{kl}\end{bmatrix} \qquad \mathbf{x} = \begin{bmatrix}x\\ y\end{bmatrix}$$

$$\mathbf{A}_{kl} = \begin{bmatrix}\cos\theta_{kl} & -\sin\theta_{kl}\\ \sin\theta_{kl} & \cos\theta_{kl}\end{bmatrix}\begin{bmatrix}\sigma_x^{-2} & 0\\ 0 & \sigma_y^{-2}\end{bmatrix}\begin{bmatrix}\cos\theta_{kl} & \sin\theta_{kl}\\ -\sin\theta_{kl} & \cos\theta_{kl}\end{bmatrix} = \mathbf{R}_{kl}^T\mathbf{D}\mathbf{R}_{kl}$$

- East and north are defined in the $+x$ and $+y$ directions, respectfully. The orientation θ is measured clockwise from east. λ is the wavelength of the kernel. σ_x and σ_y are the kernel RMS widths.
- We used prior methods to measure the wave parameters of the TEC signature; The positioning and slope the red bands in a hodochrone yields a measurement of period and phase speed. Wavelength is then derived as the product of the phase speed and period.

Chile 2015 Results

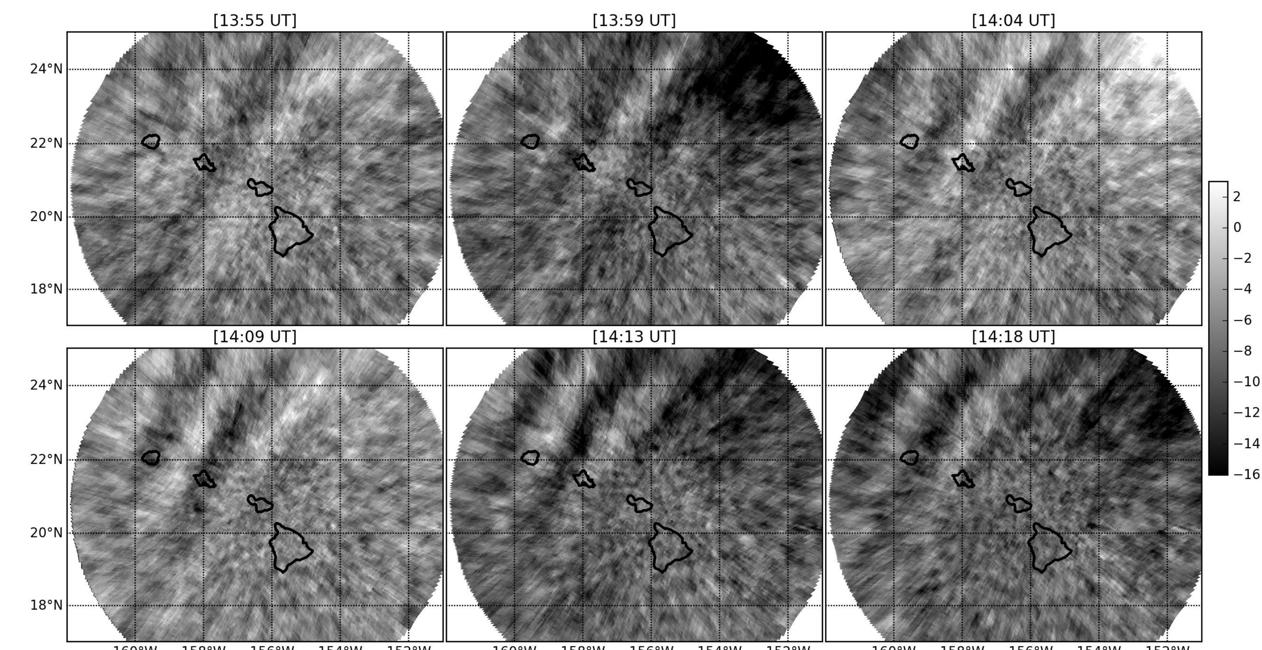

Fig. 2 All frames of the filtered 630.0 nm airglow with a visible signature during the arrival of the tsunami to Hawaii. The structure is propagating to the northwest. We used a temporal 13-tap high pass finite impulse response filter with a cutoff at 20 minutes.

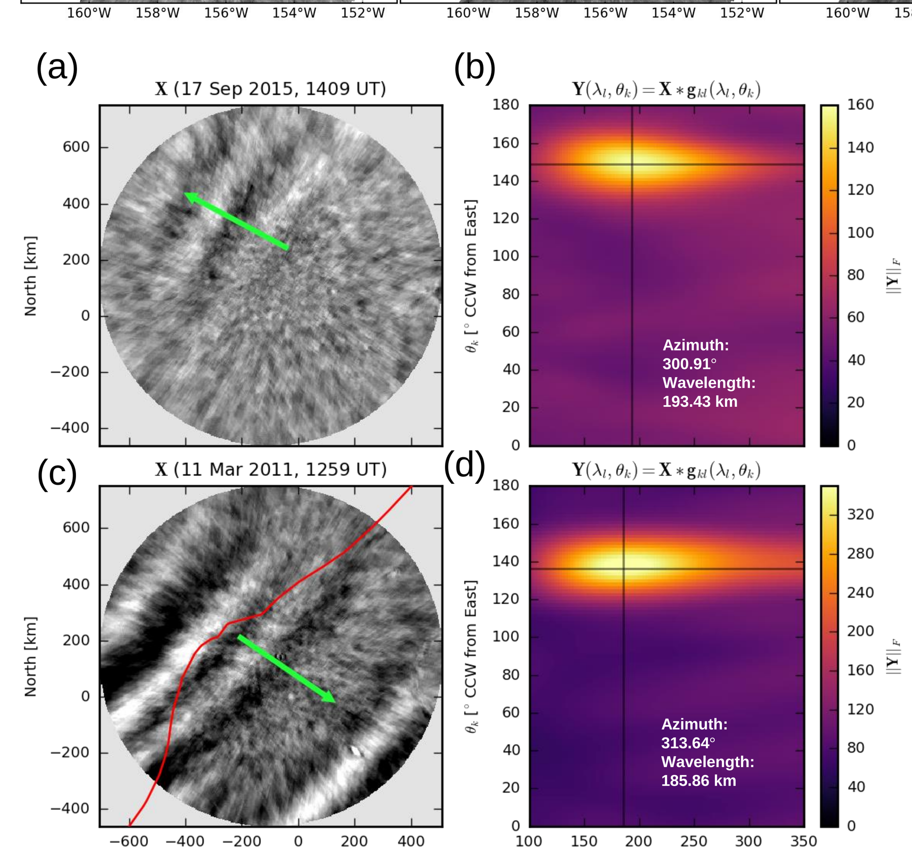

Fig. 3 (a) Filtered airglow image from the 2015 Chile event (17 September 2015, 1409 UT) input into the Gabor filter bank. The green arrow is the propagation direction. (b) Output energy surface using input in (a). (c) Filtered airglow image from the 2011 Tohoku event (11 March 2011, 1304 UT) input into the Gabor filter bank for comparison. The red line is the wavefront of the tsunami. The green arrow is the propagation direction. (d) Output energy surface using input in (c). The Tohoku results are in fairly good agreement with those reported in [1].

Chile 2015 Results (Continued)

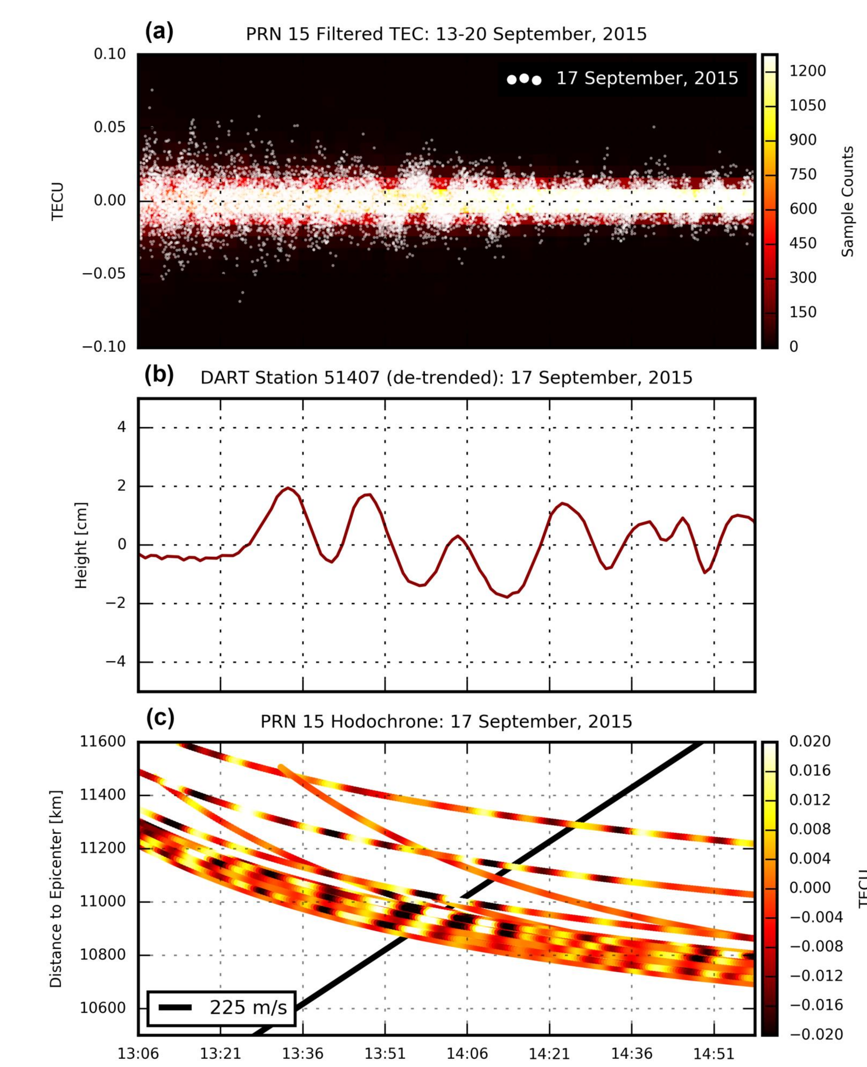

Fig 4. (a) Filtered TEC for PRN 15 from all GPS receivers in the network superimposed on top of a histogram of the filtered TEC for one week surrounding the event. Inter-receiver correlation is seen starting around 1350 UT. (b) Sea surface variation reported by DART station 51407 near Hawaii during the arrival of the tsunami. The variation had a dominant period of 14.7 minutes. The DART station is closer to Chile and reported at the ocean surface, causing it to occur roughly 25 minutes ahead of the TEC signature. (c) Hodochrone calculated using the white points in (a). The signature is seen to be propagating away from the epicenter at ~225 m/s.

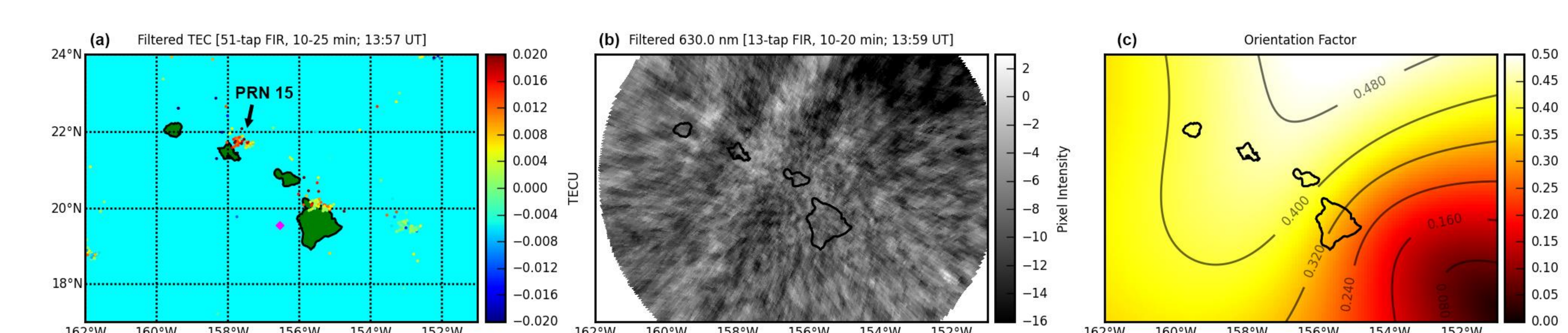

Fig. 5 Comparison of the (a) filtered TEC, (b) 630.0 nm airglow, and (c) orientation factor (a geometric model of tsunami-ionospheric coupling efficiency; see [2]) at 1357 UT (the closest airglow frame in time is shown). The signature is seen to the northwest in relatively the same location for both airglow and TEC. Notice that the orientation factor predicts the highest coupling efficiencies to the north/northwest of the receiver network.

Parameter	Airglow Measurement	TEC Measurement
Wavelength	206 km (± 3 km)	144 km (± 33.63 km)
Phase Speed	298 m/s (± 78 m/s)	225 m/s (± 21 m/s)
Period	11.9 min (± 3.26 min)	10.7 min (± 1.50 min)

Conclusions

- The location of the signatures appearing in the airglow and TEC occur downstream of the tsunami and in the maximal region of the orientation factor developed in [2]. This provides additional validation of the downstream enhancement effect.
- The TEC perturbations are weak in this event, but the location, timing and propagation direction of the signature are in fairly good agreement with the airglow observation and tsunami itself, suggesting that they are all related.
- The use of both airglow and TEC data for this event demonstrates the usefulness of multiple observation methodologies. GPS-derived TEC data typically has higher time resolution but suffers from large spatial data gaps between the different sets of raypaths for each satellite. Airglow measurements have high spatial resolution but a lower temporal resolution compared to GPS-derived TEC.